Materials Physics and Mechanics 16 (2013) 66-81 Received: December 9, 2012

PROPAGATION OF WAVES IN MICROPOLAR THERMOELASTIC SOLID WITH TWO TEMPERATURES BORDERED WITH LAYERS OR HALF-SPACES OF INVISCID LIQUID

Kunal Sharma[1*], Saurav Sharma[2], Raj Rani Bhargava[3***]**

[1]Department of Mechanical Engineering, Ecole polytechnique fédérale de Lausanne (EPFL), Lausanne, Switzerland

[2]Department of Instrumentation, Kurukshetra University, Kurukshetra, India

[3]Department of Mathematics IIT Roorkee, Roorkee 247667, India

*e-mail: kunal.sharma@epfl.ch

**e-mail: sauravkuk@gmail.com

***e-mail: rajrbfma@iitr.ernet.in

Abstract. The present study is concerned with the propagation of Lamb waves in a homogeneous isotropic thermoelastic micropolar solid with two temperatures bordered with layers or half-spaces of inviscid liquid subjected to stress free boundary conditions. The coupled thermoelasticity theory has been used to investigate the problem. The secular equations for symmetric and skew-symmetric leaky and nonleaky Lamb wave modes of propagation are derived. The phase velocity and attenuation coefficient are computed numerically and depicted graphically. The amplitudes of stress, microrotation vector and temperature distribution for the symmetric and skew-symmetric wave modes are computed numerically and presented graphically. Results of some earlier workers have been deduced as particular cases.

1. Introduction

The exact nature of layers beneath the earth's surface are unknown. Therefore, one has to consider various appropriate models for the purpose of theoretical investigation. Modern engineering structures are often made up of materials possessing an internal structure. Polycrystalline materials, materials with fibrous or coarse grain structure come in this category. Classical elasticity is inadequate to represent the behaviour of such materials. The analysis of such materials requires incorporating the theory of oriented media. For this reason, micropolar theories were developed by Eringen [1-3] for elastic solids, fluids and further for non-local polar fields and are now universally accepted. A micropolar continuum is a collection of interconnected particles in the form of small rigid bodies undergoing both translational and rotational motions.

The linear theory of micropolar thermoelasticity was developed by extending the theory of micropolar continua to include thermal effects by Eringen [4] and Nowacki [5]. Dost and Taborrok [6] presented the generalized thermoelasticity by using Green and Lindsay theory [7].

The main difference of thermoelasticity with two temperatures with respect to the classical one is the thermal dependence. Chen et al. [8, 9] have formulated a theory of heat

conduction in deformable bodies, which depend on two distinct temperatures, the conductive temperature ϕ and thermodynamic temperature θ. For time independent situations, the difference between these two temperatures is proportional to the heat supply. For time dependent problems in wave propagation the two temperatures are in general different. The two temperatures and the strain are found to have representation in the form of a travelling wave pulse, a response which occurs instantaneously throughout the body (Boley [10]). The wave propagation in the two temperature theory of thermoelasticity was investigated by Warren and Chen [11].

Various investigators Youssef [12], Puri and Jordan [13], Youssef and Al-Lehaibi [14], Youssef and Al-Harby [15], Magana and Quintanilla [16], Mukhopadhyay and Kumar [17], Roushan and Santwana [18], Kaushal et al [19], Kaushal et al. [20], Ezzat and Awad [21] and Ezzat et al. [22] studied different problems in thermoelastic and micropolar thermoelastic media with two temperature media.

For non-destructive evaluation of solid structures, the study of the interaction of elastic waves with fluid loaded solids has been recognized as a viable mean. The reflected acoustic field from a fluid-solid interface has great information, which reveals details of many characteristics of solids.

Theoretical and experimental verifications of these phenomena have been conducted for a wide variety of solids extending from the simple isotropic semi-space to the much more complicated systems of multilayered anisotropic media. Nayfeh [23] has presented a detailed review of the available literature on this subject. The influence of viscous fluid loading on the propagation of leaky Rayleigh wave in the presence of heat conduction effect was studied by Qi [24]. Subsequently, Wu and Zhu [25] suggested an alternative approach to the treatment of Qi [24]. They presented solutions for the dispersion relations of leaky Rayleigh waves when heat conduction is neglected. The same method was adopted by Zhu and Wu [26] for Lamb waves in submerged and fluid coated plates.

Nayfeh and Nagy [27] derived the exact characteristic equations for leaky waves propagating along the interfaces of several systems involving isotropic elastic solids loaded with viscous fluids, including semi- spaces and finite thickness fluid layers. The technique adopted by Nayfeh and Nagy [27] removed certain inconsistencies that unnecessarily reduce the accuracy and range of validity of the Zhu and Wu [26] results.

Various authors investigated the problem of wave propagation in micropolar thermoelastic plates e.g. Nowacki and Nowacki [28], Kumar and Gogna [29], Tomar [30, 31], Kumar and Pratap [32-37], Sharma et al. [38], Sharma and Kumar [39].

In this paper, we study the propagation of waves in an infinite homogeneous micropolar thermoelastic plate with two temperatures bordered with layers or half-space of inviscid liquid. The secular equations for different conditions of solutions have been deduced from the present one.The phase velocity and attenuation coefficient are computed numerically and depicted graphically. The amplitudes of stress, microrotation vector and temperature distribution for the symmetric and skew-symmetric wave modes are computed numerically and presented graphically for LS-theory.

2. Basic equations

Following Eringen [1] and Warren and Chen [11], the field equations in an isotropic, homogeneous, micropolar elastic medium in the context of theory of thermoelasticity with two temperatures, without body forces, body couples and heat sources, are given by

$$(\lambda+2\mu+K)\nabla\left(\nabla\cdot\vec{u}\right)-\left(\mu+K\right)\nabla\times(\nabla\times\vec{u})+K\left(\nabla\times\vec{\varphi}\right)-\nu\nabla(1-a\nabla^2)\Phi=\rho\frac{\partial^2\vec{u}}{\partial t^2}, \tag{1}$$

$$(\alpha+\beta+\gamma)\nabla\left(\nabla.\vec{\phi}\right)-\gamma\nabla\times\left(\nabla\times\vec{\phi}\right)+K\nabla\times\vec{u}-2K\vec{\phi}=\rho j\frac{\partial^2\vec{\phi}}{\partial t^2}, \tag{2}$$

$$K^*\nabla^2\Phi=\rho c^*\left(\frac{\partial}{\partial t}\right)(1-a\nabla^2)\Phi+\nu\Phi_0\left(\frac{\partial}{\partial t}\right)\left(\nabla.\vec{u}\right), \tag{3}$$

and the constitutive relations are

$$t_{ij}=\lambda u_{r,r}\delta_{ij}+\mu\left(u_{i,j}+u_{j,i}\right)+K\left(u_{j,i}-\varepsilon_{ijr}\phi_r\right)-\nu T\delta_{ij}, \tag{4}$$

$$m_{ij}=\alpha\phi_{r,r}\delta_{ij}+\beta\phi_{i,j}+\gamma\phi_{j,i}, \qquad i,j,r=1,2,3 \tag{5}$$

where ∇^2 is the Laplacian operator; λ and μ are Lame's constants; K, α, β and γ are micropolar constants; t_{ij} are the components of the stress tensor, and m_{ij} are the components of couple stress tensor; $\vec{u}$ and $\vec{\phi}$ are the displacement and microrotation vectors; ρ is the density; j is the microinertia; K^* is the thermal conductivity; c^* is the specific heat at constant strain; T is the temperature change; $\nu=(3\lambda+2\mu+K)\alpha_T$, where α_T is the coefficient of linear thermal expansio; δ_{ij} is the Kronecker delta; ε_{ijr} is the alternating symbol; T and Φ are connected by the relation $T=(1-a\nabla^2)\Phi$.

For the liquid half-space, the equation of motion and constitutive relations are given by

$$\lambda_L\nabla(\nabla.\overrightarrow{u_L})=\rho_L\frac{\partial^2\overrightarrow{u_L}}{\partial t^2}, \tag{6}$$

$$(t_{ij})_L=\lambda_L(u_{r,r})_L\delta_{ij}. \tag{7}$$

3. Formulation of the problem

Consider an infinite homogeneous isotropic, thermally conducting micropolar thermoelastic plate of thickness $2d$ initially undisturbed and at uniform temperature T_0. The plate is bordered with infinitely large homogeneous inviscid liquid half-spaces or layers of thickness h on both sides as illustrated in Figs. 1(a) and 1(b). We take origin of the co-ordinate system (x_1,x_2,x_3) on the middle surface of the plate and x_1-axis is taken normal to the solid plate.

For two dimensional problem, we take

$$\vec{u}=\left(u_1(x_1,x_3),0,u_3(x_1,x_3)\right), \qquad \vec{\phi}=\left(0,\phi_2(x_1,x_3),0\right). \tag{8}$$

For convenience, the following non dimensional quantities are introduced

$$x_1'=\frac{\omega^*x_1}{c_1}, \quad x_3'=\frac{\omega^*x_3}{c_1}, \quad u_1'=\frac{\rho\omega^*c_1}{\nu T_0}u_1, \quad u_3'=\frac{\rho\omega^*c_1}{\nu T_0}u_3,$$

$$\phi_2'=\frac{\rho c_1^{\,2}}{\nu T_0}\phi_2, \quad t'=\omega^*t, \quad T'=\frac{T}{T_0}, \quad \Phi'=\frac{\Phi}{\Phi_0}, \quad t_{ij}'=\frac{1}{\nu T_0}t_{ij}, \quad m_{ij}'=\frac{\omega^*}{c_1\nu T_0}m_{ij},$$

$$u_L'=\frac{\rho\omega^*c_1}{\nu T_0}u_L, \quad w_L'=\frac{\rho\omega^*c_1}{\nu T_0}w_L, \quad c_L^2=\frac{\lambda_L}{\rho_L}, \quad h'=\frac{c_1h}{\omega^*}, \quad d'=\frac{\omega^*d}{c_1}, \quad a'=\frac{\omega^{*2}}{c_1^2}a, \tag{9}$$

where $\omega^* = \dfrac{\rho c^* c_1^2}{K^*}$, $c_1^2 = \dfrac{\lambda + 2\mu + K}{\rho}$, ω^* is the characteristic frequency of the medium, c_L is the velocity of sound in the liquid, ρ_L is the density of the liquid, and λ_L is the bulk modulus.

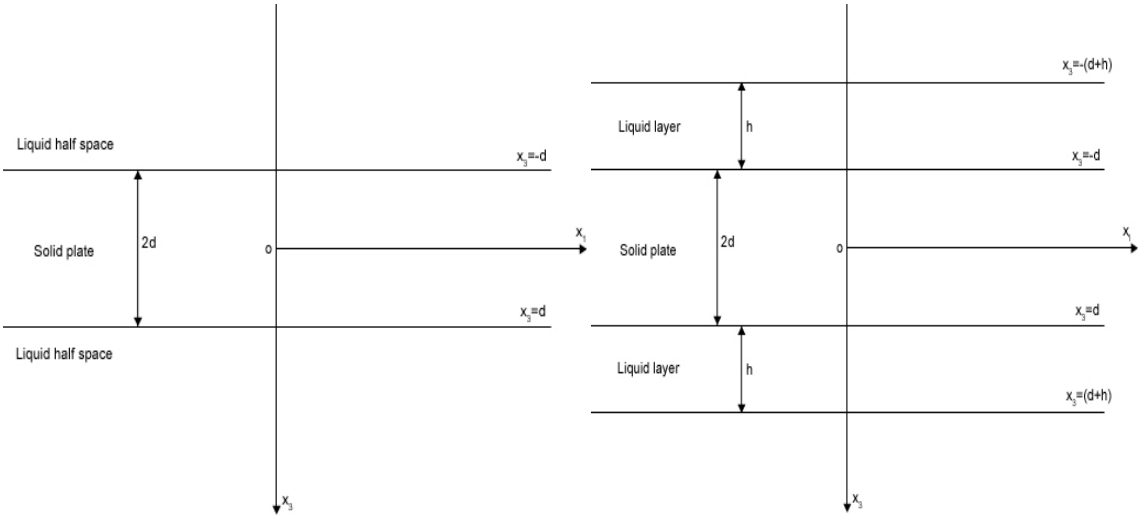

Fig. 1. Geometry of leaky Lamb waves (a) and nonleaky Lamb waves (b).

The displacement components u_1 and u_3 are related to the potential functions φ, ψ as

$$u_1 = \frac{\partial \varphi}{\partial x_1} - \frac{\partial \psi}{\partial x_3}, \qquad u_3 = \frac{\partial \varphi}{\partial x_3} + \frac{\partial \psi}{\partial x_1}. \tag{10}$$

In the liquid layers at the boundary, we have

$$u_{L_i} = \frac{\partial \phi_{L_i}}{\partial x_1} - \frac{\partial \psi_{L_i}}{\partial x_3}, \qquad w_{L_i} = \frac{\partial \phi_{L_i}}{\partial x_3} + \frac{\partial \psi_{L_i}}{\partial x_1}, \tag{11}$$

where ϕ_{L_i} and ψ_{L_i} are the scalar velocity potential components along the x_2-direction for the top liquid layer ($i=1$) and for the bottom liquid layer ($i=2$), u_{L_i} and w_{L_i} are respectively, the x_1 and x_3 components of particle velocity.

Eqs. (1)-(7) with the aid of Eqs. (8)-(11) after suppressing the primes reduce to

$$\nabla^2 \phi - p_0 (1 - a\nabla^2)\Phi - \frac{\partial^2 \phi}{\partial t^2} = 0, \tag{12}$$

$$\nabla^2 \psi + a_1 \phi_2 - a_2 \frac{\partial^2 \psi}{\partial t^2} = 0, \tag{13}$$

$$\nabla^2 \phi_2 - a_3 \nabla^2 \psi - a_4 \phi_2 - a_5 \frac{\partial^2 \phi_2}{\partial t^2} = 0, \tag{14}$$

$$\nabla^2 \Phi = a_6 \frac{\partial}{\partial t}(1 - a\nabla^2)\Phi + a_7 \left(\frac{\partial}{\partial t}\right) \nabla^2 \phi, \tag{15}$$

$$\nabla^2\phi_{L_i} - \frac{1}{\delta_L^2}\frac{\partial^2\phi_{L_i}}{\partial t^2} = 0, \quad i = 1,2, \tag{16}$$

where $a_1 = \dfrac{K}{\mu + K}$, $a_2 = \dfrac{\rho c_1^2}{\mu + K}$, $a_3 = \dfrac{Kc_1^2}{\gamma\omega^{*2}}$, $a_4 = 2\,a_3$, $a_5 = \dfrac{\hat{\rho j} c_1^2}{\gamma}$,

$a_6 = \dfrac{\rho\, c^* c_1^2}{K^*\omega^*}$, $a_7 = \dfrac{\nu^2 T_0}{\rho \mathrm{K}^*\omega^*}$, $\nabla^2 = \dfrac{\partial^2}{\partial x_1^{\,2}} + \dfrac{\partial^2}{\partial x_3^{\,2}}$, $\delta_L^2 = \dfrac{c_L^2}{c_1^2}$.

The shear motion is not supported by inviscid fluid, therefore shear modulus of liquid vanishes and hence ψ_{L_i}, $i = 1,2$ vanish. In case of inviscid liquid, the potential function layer satisfy the equation (16).

Consider the propagation of plane waves in the x_1x_3-plane with a wavefront parallel to the x_2-axis, therefore, ϕ, ψ, ϕ_2, Φ, ϕ_{L_1} and ϕ_{L_2} are independent of x_2-coordinates.
We assume the solutions of Eqs. (12)-(16) of the form

$$(\phi, \psi, \phi_2, \Phi, \phi_{L_1}, \phi_{L_2}) = \left[f_1(x_3), f_2(x_3), f_3(x_3), f_4(x_3), f_5(x_3), f_6(x_3)\right] e^{i\xi(x_1 - ct)}, \tag{17}$$

where c=$\dfrac{\omega}{\xi}$ is the non-dimensional phase velocity, ω is the frequency and ξ is the wave number.

Using Eq. (17) in Eqs. (12)-(16), we obtain

$$(\nabla^{*2} + \xi^2 c^2) f_1(x_3) = \left[1 - a\nabla^{*2}\right] f_4(x_3), \tag{18}$$

$$(\nabla^{*2} + a_6 i\xi c(1 - a\nabla^{*2})) f_4(x_3) = a_7 i\xi c\nabla^{*2} f_1(x_3), \tag{19}$$

$$(\nabla^{*2} + a_2\xi^2 c^2) f_2(x_3) = -a_1 f_3(x_3), \tag{20}$$

$$(d^2/dx_3^{\,2} - \gamma_L^{\,2}) f_k(x_3) = 0, \quad (k = 5, 6), \tag{21}$$

$$(\nabla^{*2} + a_5\xi^2 c^2) f_3(x_3) = a_3\nabla^{*2} f_2(x_3). \tag{22}$$

Eliminating $f_4(x_3)$ from Eqs. (18) and (19) and eliminating $f_3(x_3)$ from Eqs. (20) and (22) yield

$$(\nabla^{*4} + A\nabla^{*2} + B) f_1(x_3) = 0, \tag{23}$$

$$(\nabla^{*4} + C\nabla^{*2} + D) f_2(x_3) = 0, \tag{24}$$

where $\nabla^{*2} = d^2/dx_3^{\,2} - \xi^2$ and A, B, C and D are given by

$$A = \left(aa_6 - \frac{1}{\xi^2 c^2} - \frac{a_6 i}{\xi^3 c^3} - p_0 a_7 i\right) \Big/ \left(aa_6 - \frac{1}{\xi^2 c^2} - p_0 a a_7 i\right), \quad B = \left(-i\xi c a_6\right) \Big/ \left(aa_6 - \frac{1}{\xi^2 c^2} - p_0 a a_7 i\right),$$

$$C=\xi^2c^2((a_5+a_2)+\frac{a_1a_3}{\xi^2c^2}),\qquad D=a_2a_5\xi^4c^4,\qquad p_0=\frac{\Phi_0}{T_0},\qquad {\gamma_L}^2=\xi^2(1-\frac{c^2}{\delta_L^2}).$$

The roots of Eqs. (23) and (24) are given as $n_{1,2}^2=\frac{1}{2}\left[-A\pm\sqrt{A^2-4B}\right]$ and $n_{3,4}^2=\frac{1}{2}\left[-C\pm\sqrt{C^2-4D}\right].$

The appropriate potentials $\phi,\Phi,\psi,\phi_2,\phi_{L_1}$ and ϕ_{L_2}, are obtained as

$$\phi=(A_1\cos n_1x_3+A_2\cos n_2x_3+B_1\sin n_1x_3+B_2\sin n_2x_3)e^{i\xi(x_1-ct)},\tag{25}$$

$$\Phi=(h_1A_1\cos n_1x_3+h_2A_2\cos n_2x_3+h_1B_1\sin n_1x_3+h_2B_2\sin n_2x_3)e^{i\xi(x_1-ct)},\tag{26}$$

$$\psi=(A_3\cos n_3x_3+A_4\cos n_4x_3+B_3\sin n_3x_3+B_4\sin n_4x_3)e^{i\xi(x_1-ct)},\tag{27}$$

$$\phi_2=(h_3A_3\cos n_3x_3+h_4A_4\cos n_4x_3+h_3B_3\sin n_3x_3+h_4B_4\sin n_4x_3)e^{i\xi(x_1-ct)},\tag{28}$$

$$\phi_{L_1}=(E_5e^{\gamma_Lx_3}+F_5e^{-\gamma_Lx_3})e^{\iota\xi(x_1-ct)},\tag{29}$$

$$\phi_{L_2}=(E_6e^{\gamma_Lx_3}+F_6e^{-\gamma_Lx_3})e^{\iota\xi(x_1-ct)},\tag{30}$$

where $h_i=\frac{(r_1^2-n_i^2)}{p_0(1+a\xi^2+an_i^2)},\qquad h_j=\frac{({r_2}^2-n_j^2)}{a_1},$

$$n_i^2=\xi^2(c^2\alpha_i^2-1),\qquad i=1,2,3,4,\qquad r_1^2=\xi^2(c^2-1),\qquad r_2^2=\xi^2(c^2a_2-1),$$

$$\alpha_i^2=\frac{k_0\pm\sqrt{k_0^2-4a_6\tau_0k_1^{'}}}{2k_1^{'}},\ \alpha_j^2=\frac{((a_5+a_2)+\frac{a_1a_3}{\xi^2c^2})\pm\sqrt{((a_5+a_2)+\frac{a_3a_1}{\xi^2c^2})^2-4a_5a_2}}{2},$$

$$k_0=aa_6-\frac{1}{\xi^2c^2}-[\frac{a_6i}{\xi^3c^3}+p_0a_7i],\qquad k_1=\frac{aa_6}{\xi^2c^2}-\frac{1}{\xi^4c^4}-p_0aa_7i\frac{1}{\xi^3c^3},$$

$$k_1^{'}=\xi^2c^2k_1,\qquad i=1,2,\ j=3,4.$$

4. Boundary conditions

The boundary conditions at the solid-liquid interface $x_3=\pm d$ are given by:

(i) The magnitude of the normal component of the stress tensor $(t_{33})_s$ of the plate should be equal to the pressure of the liquid $(t_{33})_L$.

$$(t_{33})_s=(t_{33})_L.\tag{31}$$

(ii) The tangential component of the stress tensor should be zero.

$$(t_{31})_s=0.\tag{32}$$

(iii) The tangential component of the couple stress tensor should be zero.

$$(m_{32})_s = 0. \tag{33}$$

(iv) The normal velocity component of the solid should be equal to that of the liquid.

$$(\dot{u}_3)_s = (\dot{w})_L. \tag{34}$$

(v) The thermal boundary conditions is given by

$$\frac{\partial T}{\partial x_3} + HT = 0, \tag{35}$$

where H is the surface heat transfer coefficient. Here $H \to 0$ corresponds to thermal insulated boundaries and $H \to \infty$ refers to isothermal one.

4.1. Leaky Lamb waves. The solutions for solid media of finite thickness $2d$ sandwiched between two liquid half-spaces is given by equations (25)-(28) and

$$\phi_{L_1} = E_5 e^{\gamma_L (x_3 + d)} e^{i\xi(x_1 - ct)},\ -\infty < x_3 < -d, \tag{36}$$

$$\phi_{L_2} = F_6 e^{-\gamma_L (x_3 - d)} e^{i\xi(x_1 - ct)},\ d < x_3 < \infty. \tag{37}$$

4.2. Nonleaky Lamb waves. The corresponding solutions for a solid media of finite thickness $2d$ sandwiched between two finite liquid layers of thickness h is given by equations (25)-(28) and

$$\phi_{L_1} = E_5 \sinh \gamma_L [x_3 + (d + h)] e^{i\xi(x_1 - ct)},\ -(d + h) < x_3 < -d, \tag{38}$$

$$\phi_{L_2} = F_6 \sinh \gamma_L [x_3 - (d + h)] e^{i\xi(x_1 - ct)},\ d < x_3 < (d + h). \tag{39}$$

Nonleaky and leaky Lamb waves are distinguished by selecting the functions ϕ_{L_1} and ϕ_{L_2} in such a way that the acoustical pressure is zero at $x_3 = \mp(d + h)$. This shows that ϕ_{L_1} and ϕ_{L_2} are solutions of standing wave and travelling wave for nonleaky Lamb waves and leaky Lamb waves respectively.

5. Derivation of the dispersion equations

We apply the already shown formal solutions in this section to study the specific situations with inviscid fluid.

5.1. Leaky Lamb waves. Consider an isotropic thermoelastic micropolar plate with two temperatures completely immersed in the inviscid liquid as shown in Fig. 1(a). The thickness of the plate is $2d$ and thus the lower and upper portions of the fluid extend from $x_3 = d$ to ∞ and $x_3 = -d$ to $-\infty$ respectively. In this case, the partial waves are in both the plate and the fluid. The appropriate formal solutions for the plate and fluid are those given by equations (25)-(28), (36) and (37). By applying the boundary conditions (31)-(35) at $x_3 = \pm d$ and subsequently requiring nontrivial values of the partial wave amplitudes E_k and F_k, (k=1, 2, 3, 4), E_5, F_6 and $\gamma_L \neq 0,$ we arrive at the characteristic dispersion equations as

$$(T_1T_3)^{\pm}AT1+(T_1T_4)^{\pm}AT2+(T_2T_3)^{\pm}AT3+(T_2T_4)^{\pm}AT4+(T_3T_4)^{\pm}AT5+$$

$$+(T_3)^{\pm}AT6+(T_4)^{\pm}AT7=0 \tag{40}$$

for stress free thermally insulated boundaries ($H\to 0$) of the plate and

$$(T_1T_3)^{\pm}h_1n_2AN2-(T_1T_4)^{\pm}h_1n_2AN1-(T_2T_3)^{\pm}h_2n_1AN2+(T_2T_4)^{\pm}h_2n_1AN1+$$

$$+(T_1T_3T_4)^{\pm}h_1n_2AN3+(T_1T_2T_3)^{\pm}h_3m_6n_3AN4-(T_1T_2T_4)^{\pm}h_4n_4m_5AN4-$$

$$-(T_2T_3T_4)^{\pm}h_2n_1AN3=0 \tag{41}$$

for stress free isothermal boundaries ($H\to\infty$) of the plate.

5.2. Nonleaky Lamb waves. Consider an isotropic thermoelastic micropolar plate with two temperatures bordered with layers of inviscid liquid on both sides as shown in Fig. 1(b).

The appropriate formal solutions for the plate and fluid are given by equations (25)-(28), (38) and (39). By applying the boundary conditions (31)-(35) at $x_3=\pm d$ and subsequently requiring nontrivial values of the partial wave amplitudes E_k and F_k, (k=1, 2, 3, 4); E_5, F_6 and $\gamma_L\neq 0$, we arrive at the characteristic dispersion equations as

$$(T_1T_3)^{\pm}AT1+(T_1T_4)^{\pm}AT2+(T_2T_3)^{\pm}AT3+(T_2T_4)^{\pm}AT4+(T_3T_4)^{\pm}AT5-$$

$$-T_5(T_3)^{\pm}AT61-T_5(T_4)^{\pm}AT71=0 \tag{42}$$

for stress free thermally insulated boundaries ($H\to 0$) of the plate.

$$(T_1T_3)^{\pm}h_1n_2AN2-(T_1T_4)^{\pm}h_1n_2AN1-(T_2T_3)^{\pm}h_2n_1AN2+(T_2T_4)^{\pm}h_2n_1AN1+$$

$$+(T_1T_3T_4)^{\pm}h_1n_2AN3+(T_1T_2T_3)^{\pm}h_3m_6n_3AN4-(T_1T_2T_4)^{\pm}h_4n_4m_5AN4-$$

$$-(T_2T_3T_4)^{\pm}h_2n_1AN3=0 \tag{43}$$

for stress free isothermal boundaries ($H\to\infty$) of the plate, where

$$AT1=h_2h_3n_2n_3m_1m_6G,\ \ AT2=-h_2h_4n_2n_4m_1m_5G,\ \ AT3=h_1h_3n_1n_3m_2m_6G,$$

$$AT4=h_1h_3n_1n_3m_2m_6G,\ \ AT5=n_1n_2n_3n_4m_3QG(h_4-h_3)(h_2+h_1),$$

$$AT6=Sh_3n_3(h_2n_1-h_1n_2)(Rm_6+m_3\xi^2c),\ \ AT7=Sh_4n_4(h_1n_2-h_2n_1)(Rm_5+m_3\xi^2c),$$

$$AT61=-S(h_2n_1-h_1n_2)(Rm_6+m_3\xi^2c),\ \ AT71=-S(h_2n_1-h_1n_2)(Rm_6+m_3\xi^2c),$$

$$AN1=Sh_4n_4(Rm_5+m_3\xi^2c),\ \ AN2=Sh_3n_3(Rm_6+m_3\xi^2c),\ \ AN3=n_3n_4m_3QG(h_3-h_4),$$

$$AN4=\gamma_L(h_2m_1-h_1m_2),$$

$m_i = [d_1 l_i + d_2 n_i^2 + b_i h_i],$

$m_3 = (2d_4 + d_5) i\xi, \quad m_k = (d_4 + d_5) n_j^2 - d_4 \xi^2 - d_5 h_j, \quad i = 1,2, \quad j = 3,4, \quad k = 5,6,$

$S = \frac{\rho_L}{\rho} \xi^2 c^2, \quad R = \iota \xi c, \quad Q = \iota \xi d_2, \quad l_i = \xi^2 + n_i^2, G = -i\xi c \gamma_L, \; b_i = p_0 (1 + a\xi^2 + a n_i^2),$

$s_i = \sin m_i d, \quad s_j = \sin m_j d, \quad c_i = \cos m_i d, \quad c_j = \cos m_j d, \quad T_5 = \tanh \gamma_L h,$

$d_1 = \frac{\lambda}{\rho c_1^2}, \quad d_2 = \frac{(2\mu + \kappa)}{\rho c_1^2}, \quad d_4 = \frac{2\mu}{\rho c_1^2}, \quad d_5 = \frac{d_2}{2},$

$T_i = \tan m_i d, \quad i = 1,2,3,4.$

Here the superscript +1 refers to skew-symmetric and -1 refers to symmetric modes.

Equations (40) and (43) are the dispersion relations involving wave number and phase velocity of various modes of propagation in a micropolar thermoelastic plate with two temperatures bordered with layers of inviscid liquid or half-spaces on both sides.

6. Special cases

If the liquid layers or half-spaces on both sides are removed, then we are left with the problem of wave propagation in micropolar thermoelastic solid with two temperatures. For this, we take $\rho_L = 0$ in equations (40) and (42), the secular equations for stress free thermally insulated boundaries ($H \to 0$) for the said case reduce to

$(T_1 T_3)^{\pm} AT1 + (T_1 T_4)^{\pm} AT2 + (T_2 T_3)^{\pm} AT3 + (T_2 T_4)^{\pm} AT4 + (T_3 T_4)^{\pm} AT5 = 0.$

Subcase (i):

In this case, if $a = 0$, we obtain the secular equations in micropolar generalized thermoelastic plate.

7. Amplitudes of dilatation, microrotation and temperature distribution

In this section the amplitudes of dilatation, microrotation and temperature distribution for symmetric and skew-symmetric modes of waves have been computed for micropolar thermoelastic plate. Using Eqs. (18)-(25) and (28)-(35), we obtain

$$(e)_{sy} = [-M_1 \cos n_1 x_3 + \frac{M_2 L s_1}{s_2} \cos n_2 x_3] A_1 e^{i\xi(x_1 - ct)}, \tag{44}$$

$$(e)_{asy} = [-M_1 \sin n_1 x_3 + \frac{M_2 L c_1}{c_2} \sin n_2 x_3] B_1 e^{i\xi(x_1 - ct)}, \tag{45}$$

$$(\phi_2)_{sy} = [h_3 \sin n_3 x_1 - \frac{h_3 n_3 c_3}{n_4 c_4} \sin n_4 x_3] B_3 e^{i\xi(x_1 - ct)}, \tag{46}$$

$$(\phi_2)_{asy} = [h_3 \cos n_3 x_3 - \frac{h_3 n_3 s_3}{n_4 s_4} \cos n_4 x_3] A_3 e^{i\xi(x_1 - ct)}, \tag{47}$$

$$(T)_{sy} = [Nh_1 \cos n_1 x_3 - \frac{h_1 n_1 s_1}{n_2 s_2} N' \cos n_2 x_3] A_1 e^{i\xi(x_1 - ct)}, \tag{48}$$

$$(T)_{asy} = [Nh_1 \sin n_1 x_3 - \frac{h_1 n_1 c_1}{n_2 c_2} N' \sin n_2 x_3] B_1 e^{i\xi(x_1 - ct)}, \tag{49}$$

where

$$L = \frac{h_1 n_1}{h_2 n_2}, \quad N = (1 + a\xi^2 + an_1^2), \quad N' = (1 + a\xi^2 + an_2^2).$$

8. Numerical results and discussion

To illustrate theoretical results graphically, we now present some numerical results. The material chosen for this purpose is Magnesium crystal (micropolar elastic solid), the physical data for which is given below:

(i) *Micropolar parameters:*

$\lambda = 9.4 \times 10^{10}\, N\, m^{-2}, \quad \mu = 4.0 \times 10^{10}\, N\, m^{-2}, \quad \gamma = 0.779 \times 10^{9}\, N,$

$\kappa = 1.0 \times 10^{10}\, N\, m^{-2}, \quad \rho = 1.74 \times 10^{3}\, kg\, m^{-3}, \quad j = 2.0 \times 10^{-20}\, m^2.$

(ii) *Thermal parameters:*

$\nu = 0.268 \times 10^{7}\, N\, m^{-2} K^{-1}, \quad c^* = 1.04 \times 10^{3}\, N\, m\, kg^{-1} K^{-1},$

$T_0 = 0.298\, K, \quad K^* = 1.7 \times 10^{2}\, N\, sec^{-1} K^{-1}, \quad a = 0.5, \quad \omega = 1, \quad d = 1.0\, m.$

Numerical calculations are done by taking water as liquid and the speed of sound in water is given by $c_L = 1.5 \times 10^3 m/\sec.$

In general, wave number and phase velocity of the waves are complex quantities, therfore, the waves are attenuated in space. If we write

$$C^{-1} = V^{-1} + i\omega^{-1} Q, \tag{50}$$

then $\xi = R + iQ,$ where $R = \omega/V$ and Q are real numbers. This shows that V is the propagation speed and Q is the attenuation cofficient of waves. Using Eq. (50) in secular Eq. (40) and (42), the value of propagation speed V and attenuation cofficient Q for different modes of propagation can be obtained.

In Figures 2 to 5, LS and NLS refer to leaky and nonleaky symmetric waves in micropolar thermoelastic solid with two temperatures, LSK and NLSK refer to leaky and nonleaky skew-symmetric waves in micropolar thermoelastic solid with two temperatures, ALS and ANLS refer to leaky and nonleaky symmetric waves in micropolar thermoelastic solid, ALSK and ANLSK refer to leaky and nonleaky skew-symmetric waves in micropolar thermoelastic solid. GT represents the amplitude for micropolar thermoelatic solid with two temperatures and TS represents the amplitude for micropolar thermoelastic solid as presented in Figs. 6-8.

8.1. Phase velocity. For symmetric leaky Lamb wave modes of propagation, it is noticed that phase velocity for lowest symmetric mode for ALS remain more than the values for LS for wave number $\xi d = 2,3$ and $4 \le \xi d \le 7$ as ashown in Figs. 2(a) and 3(a). For symmetric non-leaky Lamb wave modes of propagation, the phase velocity for ALS remain greater than the values for LS for wave number $\xi d = 1$ and in the remaining range, they coincide. There is little difference in the phase velocity for LS and ALS for (n=1) symmetric leaky Lamb wave mode of propagation, the phase velocities for LS remain higher than the

velocities for ALS for wave number $\xi d = 2, 4, 5, 6, 7, 8, 10$ and for (n=1) symmetric nonleaky Lamb wave mode of propagation, the velocities for NLS and ANLS coincide. It is noticed that for (n=2) symmetric nonleaky Lamb wave modes of propagation, the phase velocitiy for NLS remain more than in case of ANLS for wave number $\xi d = 3, 5$ and the behavior is reversed for $\xi d = 2$ and in the remaining range, the phase velocities coincide for NLS and ANLS. For symmetric leaky Lamb wave mode of propagation (n=2), the phase velocities for LS remain more than the velocities for ALS for wave number $\xi d = 1, 2$ and then coincide.

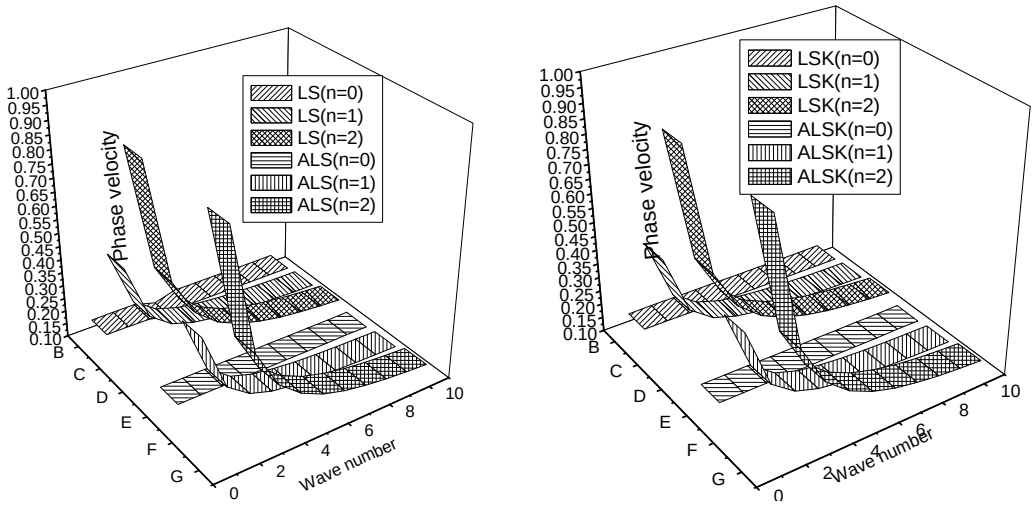

Fig. 2. Variation of phase velocity for symmetric (a) and skew-symmetric (b) leaky Lamb waves.

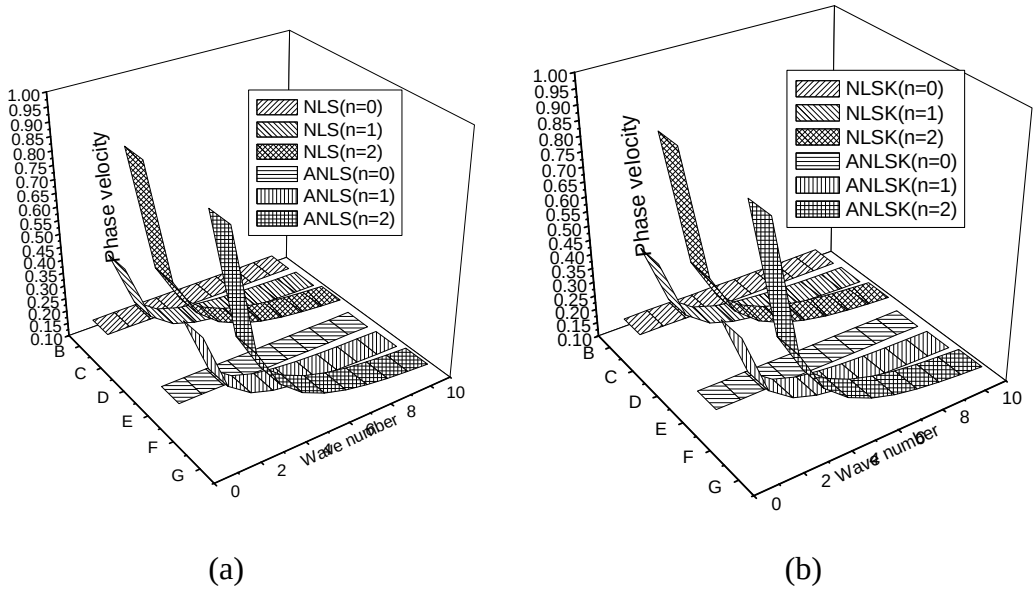

Fig. 3. Variation of phase velocity for symmetric (a) and skew-symmetric (b) nonleaky Lamb waves.

It is observed from Fig. 2(b) that the phase velocities for lowest skew-symmetric leaky Lamb wave mode of propagation for LSK and ALSK coincide.There is minute difference in

the phase velocity for LSK and ALSK for (n=1) skew-symmetric leaky Lamb wave mode of propagation for $\xi d = 1$ and for further increase in wave number the phase velocities for LS and ALS coincide. Figure 3(b) shows that for (n=1) skew-symmetric nonleaky Lamb wave mode of propagation, the velocities for ANLSK remain greater than the values for NLSK for wave number $2 \le \xi d \le 9$. It is observed that for (n=2) mode, the phase velocities for LSK are greater than the values for ALSK for $\xi d \le 2$ and for $\xi d = 3$, the behavior is reversed and with further increase in wave number, the phase velocities coincide. For (n=2) skew-symmetric mode for non leaky Lamb waves, the phase velocities for ANLSK attaingreater values for NLSK for wave number $3 \le \xi d \le 10$.

8.2. Attenuation cofficients

Figure 4(a) shows that for symmetric leaky Lamb wave mode (n=0), the magnitude of attenuation cofficient for LS remain more than the value of attenuation cofficient for ALS in the whole region. For (n=1) symmetric mode, the values for LS remain more than the values for ALS in the whole region, except for $\xi d = 1$. It is observed that for (n=2) symmetric mode the phase velocities for LS remain more than the values for ALS in the whole region,except for $\xi d = 2$. The values of attenuation cofficient for (n=2) mode for LS and ALS are magnified by afactor of 100. Figure 4(b) depicts that the magnitude of attenuation for (n=0) mode for LSK attain maximum value 0.00024 at $\xi d = 2$ and ALSK attain greater values as compared to the values for LSK for $7 \le \xi d \le 9$. For (n=1) skew-symmetric mode, the values for LSK remain slightly more than the values for ALSK for wave number $2 \le \xi d \le 5$ and $7 \le \xi d \le 10$. It is observed that for (n=2) mode, the magnitude of attenuation cofficient for LSK remain more than in case of ALSK in the whole region.

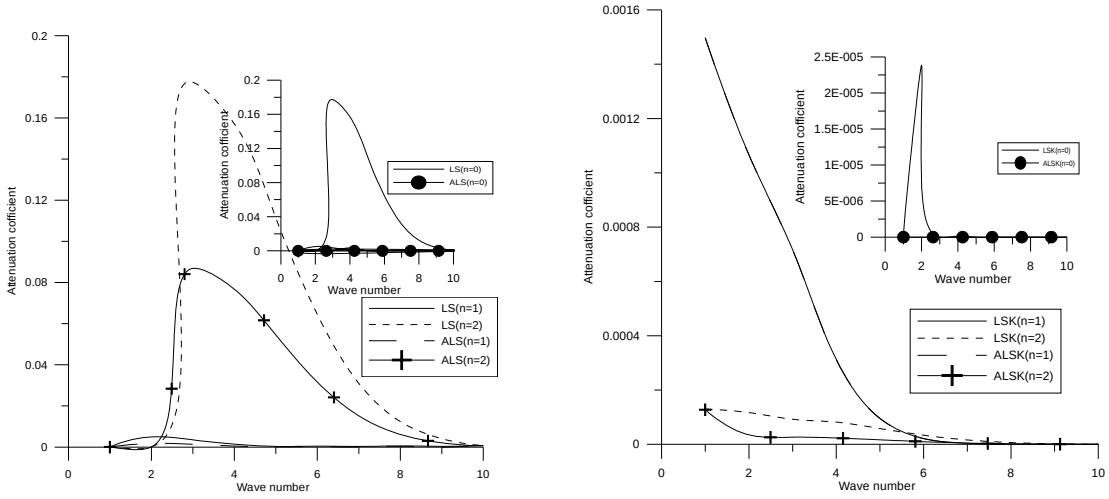

Fig. 4. Variation of attenuation coefficient for symmetric (a) and skew-symmetric (b) leaky Lamb waves.

It is evident from Fig. 5(a) that for symmetric nonleaky Lamb wave mode (n=0), the attenuation cofficient for NLS remain greater than the values for ANLS in the whole region, except for $\xi d = 1$. It is noticed that for (n=1), the magnitude of attenuation cofficient for NLS and ANLS attain maximum value at $\xi d = 1$. For (n=3) mode, the values for NLS and ANLS decrease in the whole region.

It can be concluded from Fig. 5(b) that for (n=0) skew-symmetric nonleaky Lamb wave mode of propagation, the magnitude of attenuation cofficient for NLSK attain maximum

value of 0.0145 at $\xi d = 2$ and ANLSK attain maximum valu at $\xi d = 4$. It is observed that for (n=1), the magnitude for NLSK remain more than the values for ANLSK in the region $2 \le \xi d \le 8$ and the behavior is reversed in the remaining region. For (n=2) mode, NLSK attain maximum value 0.0428 and ANLSK attain maximum value of 0.0250 at $\xi d = 3$.

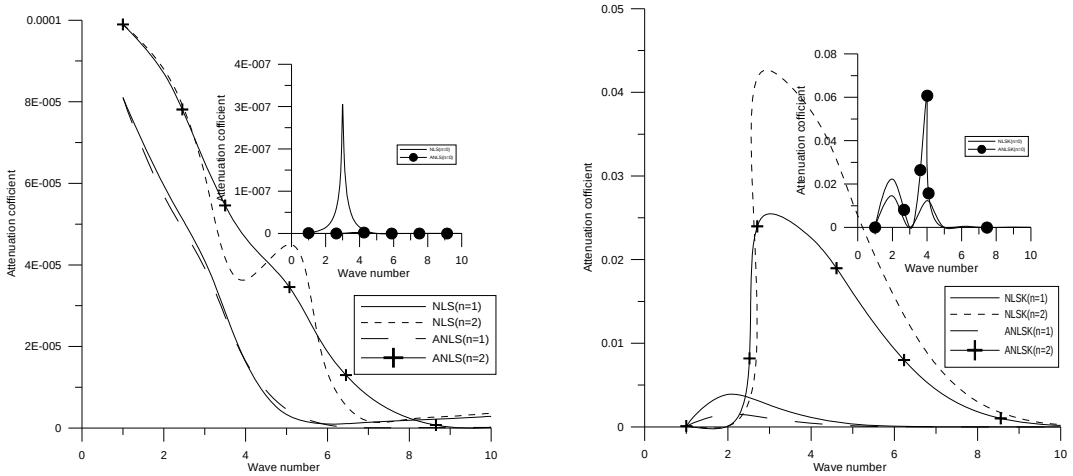

(a) (b)

Fig. 5. Variation of attenuation coefficient for symmetric (a) and skew-symmetric (b) nonleaky Lamb waves.

8.3. Amplitudes. TS represents the amplitude for micropolar thermoelastic solid and GT represents the amplitude for micropolar thermoelastic solid with two temperatures in Figs. 6 to 8.

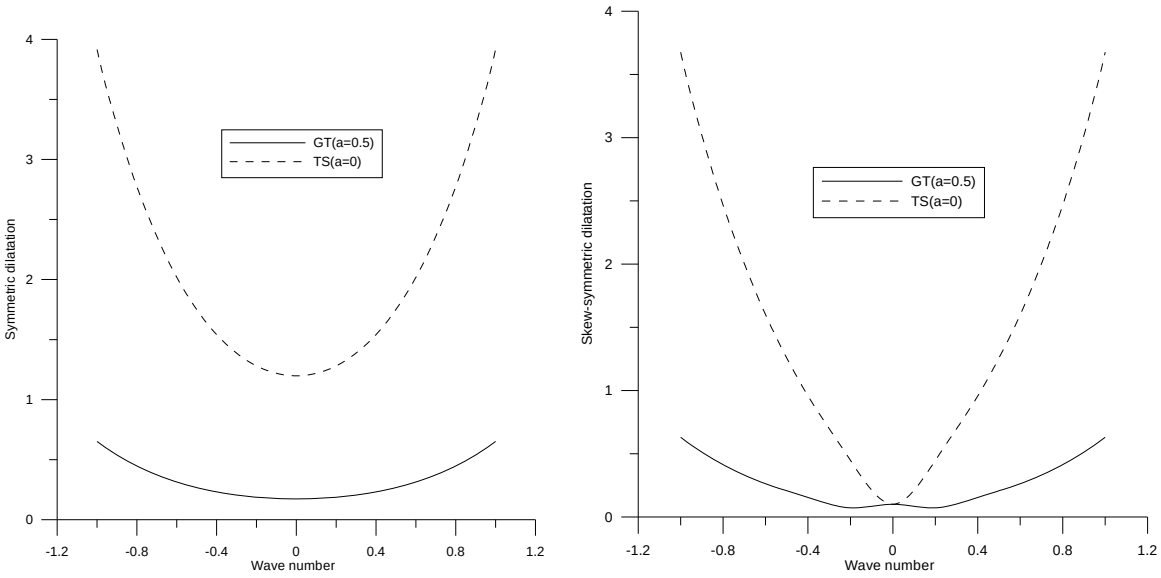

(a) (b)

Fig. 6. Variation of symmetric (a) and skew-symmetric (b) dilatation.

Variations of symmetric and skew-symmetric amplitudes of dilatation for LS theory for stress free thermally insulated boundary are depicted in Figs. 6(a) to 6(b). The dilatation is

minimum at the centre and maximum at the surfaces for symmetric and skew-symmetric modes. Also the dilatation for TS remain more than the dilatation for GT in the whole region.

It is evident from Fig. 7 that the amplitude of symmetric microrotation is minimum at the centre and the surfaces and attain maximum value in the region between centre and surface. The amplitude of skew-symmetric microrotation is maximum at the surfaces.

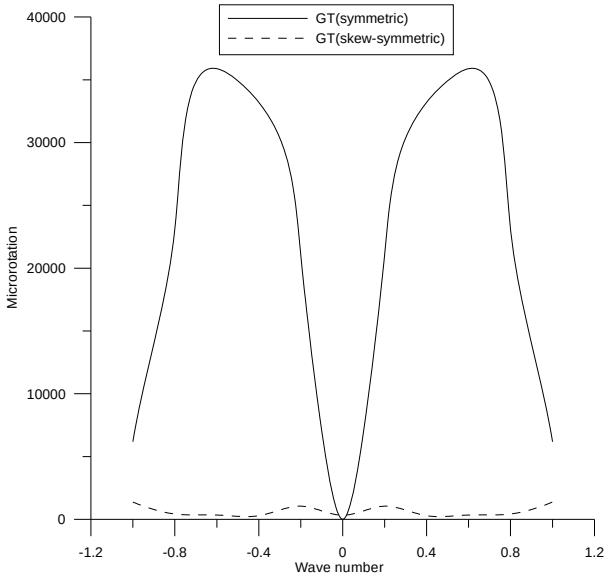

Fig. 7. Variation of symmetric and skew-symmetric microrotation.

The amplitude of symmetric and skew-symmetric temperature attains least value at the centre and maximum at the surfaces as shown in Figs. 8(a) and 8(b). Also the ampiltude of symmetric temperature for TS is greater than that for GT, while the amplitude of skew-symmetric temperature for GT is greater than that for TS.

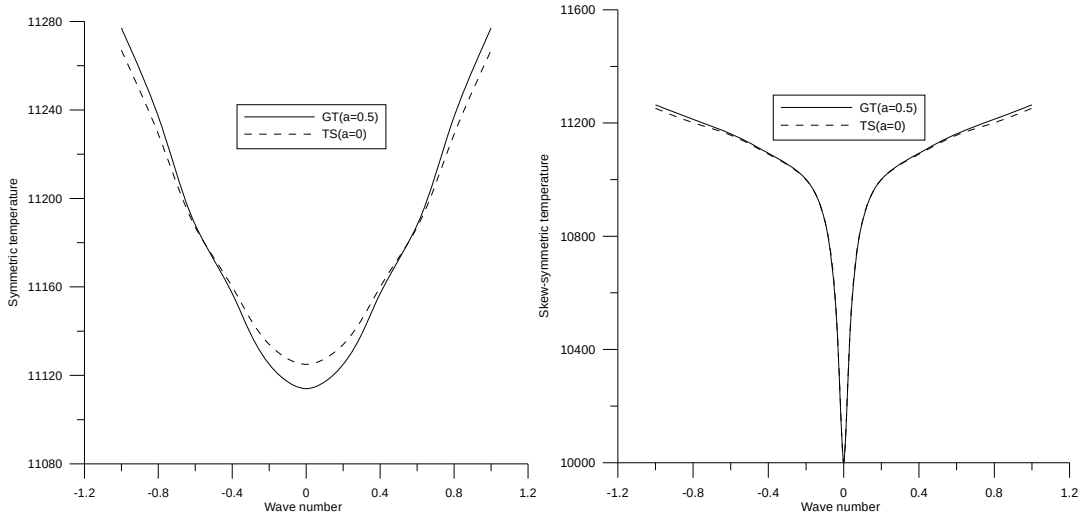

(a) (b)

Fig. 8. Variation of symmetric (a) and skew-symmetric (b) temperatures.

9. Conclusions

It is noticed that the variation of phase velocities of lowest symmetric and skew-symmetric mode for leaky and non leaky Lamb waves show slight fluctuation in the intermediate range

and then coincide with increase in wave number. Also the phase velocities for higher symmetric and skew-symmetric mode attain peak value at vanishing wave number and as wave number increases the phase velocities decrease sharply. The values of attenuation cofficient of (n=2) skew-symmetric leaky and nonleaky Lamb waves mode for TWST remain higher than that in case of TS. It is also noticed that the values of attenuation cofficient for lowest symmetric and skew-symmetric mode for leaky and non leaky Lamb waves are very small as compared to the values for highest mode. The values of symmetric and skew-symmetric dilatation in case of TS are greater in comparison to that of GT and the values of symmetric temperature in case of TS are higher than that in case of GT, while the values of skew-symmetric temperature in case of TS are higher.

References

[1] A.C. Eringen // *J. Math. Mech.* **15** (1966) 909.
[2] A.C. Eringen // J. *Math. Mech.* **16 (**1966**)** 1.
[3] A.C. Eringen, In: *Continuum Physics*, ed. by A.C. Eringen (Academic Press, New York, 1976), Vol. IV, p. 205.
[4] A.C. Eringen, *Foundations of micropolar thermoelasticity*, International Centre for Mechanical Science, Udline Course and Lectures 23 (Springer-Verlag, Berlin, 1970).
[5] W. Nowacki, *Theory of Asymmetric Elasticity* (Pergamon, Oxford, 1986)
[6] S. Dost, B. Taborrok // *Int. J. Eng. Sci.* **16** (1978) 173.
[7] A.E. Green, K.A. Lindsay // *J. of Elasticity* **2** (1972) 1.
[8] P.J. Chen, M.E. Gurtin, W.O. Williams // *Zeitschrift für angewandte Mathematik und Physik **19*** (1968) 960.
[9] P.J. Chen, M.E. Gurtin, W.O. Williams // *Zeitschrift für angewandte Mathematik und Physik* **20** (1969) 107.
[10] M. Boley // *J. Appl. Phys.* **27** (1956) 240.
[11] W.E. Warren, P.J. Chen // *Acta Mechanica* **16** (1973) 21.
[12] H.M. Youssef // *IMA Journal of Applied Mathematics* **71** (2006) 383.
[13] P. Puri, P. Jordan // *Int. J. of Eng. Sci.* **44** (2006) 1113.
[14] H.M. Youssef, E.A. Al-Lehaibi // *Int. J. of Solid and Struct*. **44** (2007) 1550.
[15] H.M. Youssef, H.A. Al-Harby // *Archive Applied Mechanics* **77** (2007) 675.
[16] A. Magana, R. Quintanilla // Math. and Mech. of Solids, Online (2008).
[17] S. Mukhopadhyay, R. Kumar // *J. of Thermal Stresses* **32** (2009) 341.
[18] K. Roushan, M. Santwana // *Int. J. Eng. Sci.* 48 (2010) 128-139.
[19] S. Kaushal, N. Sharma, R. Kumar // *Int. J. of Appl. Mech. and Eng.* **15** (2010) 1111.
[20] S. Kaushal, R. Kumar, A. Miglani // *Mathematical Sciences* **5** (2011) 125.
[21] M.A. Ezzat, E.S. Aiwad // *J. of Thermal Stresses* **33** (2010) 226.
[22] M.A. Ezzat, F. Hamza, E. Awad // *Acta Mechanica Solida Sinica* **23** (2010) 200.
[23] A.H. Nayfeh, *Wave Propagation in Layered Anisotropic Media: With Application to Composites* (Elsevier Science, North-Holland, 1995)
[24] Q. Qi // *Journal of Acoustical Society of America* **95** (1994) 3222.
[25] J. Wu, Z. Zhu // *Journal of Acoustical Society of America* **97** (1995) 3191.
[26] Z. Zhu, J. Wu // *Journal of Acoustical Society of America* **98** (1995)1059.
[27] A.H. Nayfeh, P.B. Nagy // *Journal of Acoustical Society of America* **101** (1997) 2649.
[28] W. Nowacki, W.K. Nowacki // *Bulletin de L'Academie Polonaise Des Science: Série des sciences techniques* **17** (1969) 45.
[29] R. Kumar, M.L. Gogna // *Int. J. of Eng. Sci.* **27** (1988) 89.
[30] S.K. Tomar // *Proceedings of the National Academy of Sciences, India Section A: Physical Sciences* **72** IV (2002) 339.
[31] S.K. Tomar // *J. of Vibration and Control* **11** (2005) 849.

[32] R. Kumar, G. Pratap // *Appl. Math. and Mech.* **27** (2006) 1049.
[33] R. Kumar, G. Pratap // *Int. J. of Appl. Mech. and Eng.* **12** (2007) 655.
[34] R. Kumar, G. Pratap // *Buletinul Institutului Politehnic din Iaşi* **3-4** (2007) 53.
[35] R. Kumar, G. Pratap // *Int. J. of Appl. Math. and Mech*. **4** (2008) 19.
[36] R. Kumar, G. Pratap // *Appl. Math. and Inf. Sci.* **5** (2009) 39.
[37] R. Kumar, G. Pratap // *Appl. Math. and Inf. Sci.* **4** (2010) 107.
[38] J.N. Sharma, S. Kumar, Y.D. Sharma // *J. of Thermal Stresses* **31** (2008) 18.
[39] J.N. Sharma, S. Kumar // *Meccanica* **44** (2009) 305.